

# Lab on a Chip

Accepted Manuscript



This is an *Accepted Manuscript*, which has been through the Royal Society of Chemistry peer review process and has been accepted for publication.

*Accepted Manuscripts* are published online shortly after acceptance, before technical editing, formatting and proof reading. Using this free service, authors can make their results available to the community, in citable form, before we publish the edited article. We will replace this *Accepted Manuscript* with the edited and formatted *Advance Article* as soon as it is available.

You can find more information about *Accepted Manuscripts* in the [Information for Authors](#).

Please note that technical editing may introduce minor changes to the text and/or graphics, which may alter content. The journal's standard [Terms & Conditions](#) and the [Ethical guidelines](#) still apply. In no event shall the Royal Society of Chemistry be held responsible for any errors or omissions in this *Accepted Manuscript* or any consequences arising from the use of any information it contains.

## **Polydimethylsiloxane-polycarbonate hybrid microfluidic device capable of generating perpendicular chemical and oxygen gradients for cell culture studies**

Chia-Wen Chang<sup>a,1</sup>, Yung-Ju Cheng<sup>a,1</sup>, Melissa Tu<sup>b</sup>, Ying-Hua Chen<sup>a</sup>, Chien-Chung Peng<sup>a</sup>, Wei-Hao Liao<sup>a</sup>, and Yi-Chung Tung<sup>a,\*</sup>

<sup>a</sup>*Research Center for Applied Sciences, Academia Sinica, Taipei 11529, Taiwan*

<sup>b</sup>*Princeton University, Princeton, NJ 08544, USA*

\*Corresponding author. Tel: +886 2 27873138

E-mail: [tungy@gate.sinica.edu.tw](mailto:tungy@gate.sinica.edu.tw) (Y.-C. Tung)

<sup>1</sup>These authors contribute equally to this work

### **Abstract**

This paper reports a polydimethylsiloxane-polycarbonate (PDMS-PC) hybrid microfluidic device capable of performing cell culture under combinations of chemical and oxygen gradients. The microfluidic device is constructed by two PDMS layers with microfluidic channel patterns separated by a thin PDMS membrane. The top layer contains an embedded PC film and a serpentine channel for spatially confined oxygen scavenging chemical reaction to generate oxygen gradient in the bottom layer for cell culture. Using the chemical reaction method, the device can be operated with small amount of chemicals without bulky gas cylinders and sophisticated flow control schemes. Furthermore, it can be directly used in conventional incubators with syringe pumps to simplify the system setup. The bottom layer contains arrangements of serpentine channels for chemical gradient generation and a cell culture chamber in downstream. The generated chemical and oxygen gradients are experimentally characterized using fluorescein solution and oxygen-sensitive fluorescence dye, respectively. For demonstration, 48-hour cell-based drug testing and cell migration assay using human lung adenocarcinoma epithelial cell (A549) are conducted under various combinations of chemical and oxygen gradients in the experiments. Drug testing results show the increase of A549 cell apoptosis due to the hypoxia-activated cytotoxicity of Tirapazamine (TPZ), and also suggest great cell compatibility and gradient controllability of the device. In addition, A549 cell migration assay results demonstrate aerotactic behavior of A549 cells, and suggest

oxygen gradient plays an essential role to guide cell migration, and the migration results under combinations of chemokine and oxygen gradients cannot be simply superposed from the single gradient results. The device is promising to advance *in vitro* microenvironments control to better study cellular responses under various physiological conditions for biomedical applications.

*Keywords:* Cell culture; Polydimethylsiloxane; Polycarbonate; Chemical gradient; Oxygen gradient; Drug testing; Cell migration

## 1. Introduction

Recently, engineering various gradients has drawn extensive attentions for biomedical applications because gradients play essential roles in many biological activities and regulate a number of cellular functions *in vivo*. Chemical gradients have been shown to affect various cell behaviors such as migration, proliferation, and differentiation during development, wound healing, inflammation, and tumorigenesis<sup>1, 2</sup>. For instance, a neutrophil chooses its direction of polarity and movement in response to chemokine gradients, named chemotaxis<sup>2</sup>. Oxygen tension in physiological conditions is essential for cellular activities, such as cell growth, survival and migration, suggesting its important functions for modulating cell fates<sup>3, 4</sup>. Moreover, modulating oxygen tensions is also important for tissue repair and regeneration. For example, human endothelial cells are influenced by a wide range of oxygen microenvironments in human bodies, and oxygen tensions can regulate gene expression in cells<sup>5, 6</sup>. Therefore, it is crucial to investigate the effect of oxygen tensions on cellular behaviors of interest for further clinical research and applications.

Over the past few years, many tools and technologies have been developed to create various spatiotemporal gradients for cell studies<sup>7</sup>. Microfluidics is one of the most promising techniques, due to its great controllability in both spatial and temporal domains<sup>8, 9</sup>. A number of microfluidic device have been developed to create physical and biochemical microenvironments for various biomedical applications<sup>10-20</sup>. Furthermore, recent development of microfluidic devices with single gradient has greatly promoted stable investigations for cellular behaviors at micrometer resolution. For example, a chemical gradient generating microfluidic device based on

arrangements of serpentine channels can make cells expose to concentration gradients of growth factors under continuous flow, and the cellular responses are comparable to those measured using traditional cell culture plates<sup>21</sup>. In addition, a similar microfluidic device design can also be used to generate oxygen gradients by delivering gases with different nitrogen/oxygen mixing ratios *via* diffusion. By providing rapid and controllable oxygen gradients, the devices greatly improve oxygen-based culturing methods for *in vitro* cell studies<sup>9, 22</sup>. Nevertheless, using mixed oxygen/nitrogen gases for oxygen gradient generation requires precise flow control instruments, tedious interconnections, and bulky gas cylinders to store compressed gases. Moreover, the gas may alter local CO<sub>2</sub> concentrations and cause bubble generation inside the microfluidic channels for cell culture, which makes the method not suitable for long-term experiments. Recently, a single-layer microfluidic device capable of generating oxygen gradients using spatially confined oxygen generation or scavenging chemical reactions is constructed. The device can be directly applied for cell culture in conventional cell incubators for various cellular biology studies under oxygen gradients without complicated instrumentation<sup>23, 24</sup>.

The presence of multiple gradients in physiological microenvironments shows great influences on cellular behaviors has led scientists to focus on integration of multiple gradients in microfluidic systems for *in vitro* investigation. However, current integrated systems face several challenges that retard their practical usage for biology studies. For instance, complicated device architectures and sophisticated instrumentation are usually required to generate combinations of both chemical and oxygen gradients. Recently, a single-layer microfluidic device is constructed to combine oxygen and chemical gradients for cell studies<sup>25</sup>. However, the oxygen gradients generated in the device are controlled by direct addition of oxygen scavenger into the growth medium. The chemical addition can alter the medium compositions, and further affect cellular responses<sup>26</sup>. Moreover, the oxygen gradient profile cannot be well predicted and controlled since it only relies on oxygen diffusion through the entire device.

This paper reports a microfluidic cell culture device capable of simultaneously generating stable perpendicular chemical and oxygen gradients with long-term stabilities, great cell incubator compatibility and straightforward instrumentation. The

entire microfluidic device is made of an elastomeric material, polydimethylsiloxane (PDMS), with an embedded polycarbonate (PC) film as a gas diffusion barrier. PDMS has been broadly exploited to construct microfluidic devices due to its great gas permeability, optical transparency, and manufacturability<sup>27</sup>. The device can generate chemical gradients using the well-developed channel design based on arrangements of serpentine channels, and generate oxygen gradient using the previously developed spatially confined chemical reaction method<sup>23,24,28</sup>. As a result, the designed device can be simply actuated by syringe pumps without bulky gas cylinders and sophisticated flow control schemes, which greatly reduce the instrumentation complexity. Due to the spatial confinement of chemical reactions, the usage of chemicals can be minimized without altering compositions of culture medium. In addition, the entire experimental setup can be directed placed in conventional cell incubators for optimized cell culture conditions.

In this paper, the generated chemical and oxygen gradients are numerically simulated and experimentally characterized. In the cell experiments, carcinomic human alveolar basal epithelial (A549) cells are cultured in the microfluidic device for demonstration. The developed device is first employed for drug testing to evaluate the device biocompatibility and study cell viability under combinations of anti-tumor drug (Tirapazamine, TPZ) and oxygen gradients. Furthermore, cell migration studies under various combinations of chemokine (stromal cell-derived factor 1, SDF-1 $\alpha$ ) and oxygen gradients are performed to demonstrate the device functionalities. The results show both gradients can be stably generated in the device and exploited for drug testing and cell migration studies. Consequently, the developed device provides an easy-to-operate yet powerful platform to better investigate cellular responses under various chemical and oxygen gradient combinations.

## 2. Materials and methods

### 2.1. Device design and fabrication

The device is constructed by two PDMS layers: top layer for spatially confined chemical reactions to generate oxygen gradients in the cell culture chamber,

and bottom layer for the generation of chemical gradient with a cell culture chamber in downstream. A PDMS membrane with thickness of 100  $\mu\text{m}$  is sandwiched between the two layers to prevent the chemicals in the top layer directly contact the cell culture medium. The channel heights are 100  $\mu\text{m}$  for both top and bottom layers. In order to generate chemical gradients, two inlets and a series of serpentine channels is placed before the cell culture chamber<sup>29</sup>. In the experiment, the device contains 4 sets of parallel-arranged serpentine channels with same geometries to generate 6 different concentrations across the width of the channel. The chemical gradients can be manipulated by designing the geometries of the channels.

The oxygen gradient is generated by the spatially confined oxygen scavenging chemical reaction in the top channel microfluidic channel previously developed in our lab<sup>23, 24</sup>. The chemical reaction method can generate oxygen gradients inside the microfluidic without using bulky gas cylinders, tedious interconnections, and sophisticated gas flow control schemes. The oxygen gradient profiles can be further controlled by altering chemical reaction rates using different concentrations of chemicals<sup>23, 24</sup>. In order to make oxygen scavenging more efficient for larger cell culture chamber, a PC film with thickness of 1 mm is embedded into the top PDMS layer. PC has a lower oxygen diffusion coefficient ( $D = 8.0 \times 10^{-12} \text{ m}^2/\text{s}$ ) than that of a PDMS ( $D = 4.0 \times 10^{-9} \text{ m}^2/\text{s}$ ), which can efficiently minimize the oxygen diffusion through the top layer from ambient<sup>30</sup>. In addition, due to the spatial confinement of the chemical reaction, oxygen gradient can be stably and efficiently generated with minimal chemical requirements, and the device possesses great compatibility to conventional cell incubators. Therefore, all the experiments can be performed inside cell incubators without complicated instrumentation, which are highly desired in biological laboratories. In the experiments, the reduction of an organic compound, pyrogallol (benzene-1,2,3-triol,  $\text{C}_6\text{H}_6\text{O}_3$ ), is exploited for oxygen scavenging<sup>31</sup>. In the chemical reaction, pyrogallol absorbs oxygen rapidly in alkaline solution. Pyrogallol and sodium hydroxide (NaOH) are introduced into the top channel from two inlets separately. Two chemicals mix and react with each other within the serpentine channel right before flowing in to the channel on top of the cell culture chamber located in the bottom layer. Oxygen in the bottom channel diffuses through the PDMS membrane and reacts with pyrogallol to reduce oxygen tension in the upstream

of the cell culture chamber and generate oxygen gradient along the perfusion flow direction.

The device is fabricated using the well-developed multilayer soft lithography (MSL) replica molding process<sup>16,32</sup>. Fig. 1(a) shows the schematic of the fabrication process. In brief, the master molds with positive relief features are fabricated by patterning negative tone photoresist (SU-8 2050, MicroChem Co., Newton, MA) on silicon wafers using conventional photolithography techniques. The molds are then silanized with 1H,1H,2H,2H-perfluorooctyltrichlorosilane (78560-45-9, Alfa Aesar, Ward Hill, MA) in a desiccator for 45 minutes at room temperature to prevent undesired bonding between PDMS and the molds. PDMS precursor is prepared by mixing base and curing agent with ratio of 10:1 (v/v). For top layer with an embedded PC layer, small amount of PDMS precursor (approximately 5 g) is poured on the mold and cured at 60°C for more than 5 hours first. A PC film (Quantum Beam Technologies Co., Tainan, Taiwan) with thickness of 1 mm is then placed on top of the cured PDMS layer. Afterwards, PDMS precursor is poured on top of the PC film, and the entire device is cured at 60°C for another 5 hours in a vacuum oven to ensure the seamless attachment between PDMS and the PC film. The bottom layer is fabricated by pouring the PDMS precursor on the mold, and the PDMS membrane is prepared by spinning the aforementioned PDMS precursor on top of a silanized silicon wafer. To assemble the device, the PDMS membrane is bonded to the top layer using oxygen plasma surface treatment at 90W for 40 s (PX-250, Nordson MARCH Co., Concord, CA). Four inlets (two for the top layer; and two for the bottom layer) and two outlets (one for each layer) with diameters of 2 mm are punched through the bonded layer using a biopsy punch. The assembled layer is then bonded to the bottom layer using the same oxygen plasma surface treatment. The entire fabricated device is then placed in a 60°C oven for 5 hours to promote the bonding strength and cell compatibility. Fig. 1(b) shows the photo of the fabricated microfluidic device filled with colored food dyes.

## 2.2. Generation and characterization of chemical gradients

In the designed device, the chemical gradient is generated across the width of the cell culture chamber, which is perpendicular to the perfusion flow direction. To

characterize the chemical concentration profiles generated in the microfluidic device, fluorescein sodium salt solution (F6300, Sigma-Aldrich Co., St Louis, MO) and distilled water are introduced into the channel at the bottom layer from the two separate inlets. Fluorescence images of the cell culture chamber are captured using an inverted fluorescence microscope (AF7000, Leica Microsystems Ltd., Germany). The fluorescein concentration profiles across the width of the cell culture chamber are estimated by analyzing the fluorescence intensities of the captured images using an image analysis software, ImageJ (Ver. 1.47, National Institute of Health, Bethesda, MD). The upstream, midstream and downstream are defined as the position of 0, 1.5 and 3.0mm from the beginning of measurement region down the chamber. In order to predict the generated gradients for various chemicals, a numerical simulation is performed using COMSOL Multiphysics software (Ver. 4.3b, COMSOL Inc., Burlington, MA) as shown in Fig. 2(a) for comparison.

### 2.3. Generation and characterization of oxygen gradients

The oxygen gradient is generated along the cell culture chamber, which is parallel to the perfusion flow direction in the designed device. The oxygen gradient is generated using the previously developed spatially confined chemical reaction method. The oxygen scavenging chemical reaction is accomplished using pyrogallol (87-66-1, Alfa Aesar, Ward Hill, MA) and NaOH(30620, Sigma-Aldrich, St Louis, MO)<sup>23</sup>. To calibrate the generated oxygen gradients, an oxygen sensitive fluorescence dye, tris (2,2'-bipyridyl) ruthenium (III) chloride, hexahydrate, (50525-27-4, Acros Organics, Geel, Belgium) is exploited in the experiments<sup>33, 34</sup>. According to Stern-Volmer equation, the fluorescence intensity of the dye is reduced when reacting with oxygen as:

$$I_0/I = 1 + K_q[\text{O}_2] \quad (1)$$

Where  $I$  is the fluorescence intensity in the presence of oxygen,  $I_0$  is the fluorescence intensity without oxygen, and  $K_q$  is the quenching constant. Therefore, the oxygen gradient profiles can be estimated by measuring the fluorescence intensities. The middle described in Fig. 3(b) is the position in the middle across the width of the entire cell culture chamber. The left and right are the positions 1.5 mm away from the



middle, respectively. The detail calibration process is described in our previous paper<sup>23</sup>. In the experiments, the fluorescence intensities are measured by analyzing the fluorescence images captured using the inverted fluorescence microscope.

#### 2.4. Cell culture

To demonstrate applications of the developed device for cell culture, carcinomic human alveolar basal epithelial cells (A549, ATCC, Manassas, VA) are utilized for the experiments conducted in this paper. A549 cells are cultured in F-12K medium (Gibco 21127, Invitrogen Co., Carlsbad, CA) with 10% v/v fetal bovine serum (FBS) (Gibco 10082, Invitrogen) and 1% v/v antibiotic–antimycotic (Gibco 15240, Invitrogen). The stocks are maintained under 5% CO<sub>2</sub> in T75 cell culture flasks (Nunc 156367, Thermo Scientific Inc., Rochester, NY), and passaged by dissociation with 0.25% trypsin-EDTA (Gibco 25200, Invitrogen).

#### 2.5. Drug testing

The device is first exploited to perform drug testing on A549 cells with various drug concentrations and under different oxygen tensions. In the experiments, an anti-cancer drug, Tirapazamine (TPZ), which is activated to a toxic radical only at very low levels of oxygen, is tested<sup>35, 36</sup>. Cell suspensions for the experiments are prepared by centrifugation of dissociated cells at 1000 rpm for 3 min at room temperature. The microfluidic channel with a cell culture chamber is treated with extracellular matrix (ECM) protein, fibronectin (F2006, Sigma-Aldrich Co., St Louis, MO), at a concentration of 50 µg/ml overnight inside an incubator before introducing the cell suspension into the microfluidic device. 200 µl of the cell suspension with density of 2,000 cells/µl is then introduced into the device, and incubated for more than 2 hours to promote cell adhesion onto the PDMS substrate. After cell attachment, the cells are cultured for 24 hours inside the microfluidic channel with continuous medium perfusion at a flow rate of 1 µl/min. The cells are then stained with 5 µM CellTracker™ Blue CMAC (7-Amino-4-Chloromethylcoumarin) (C2110, Invitrogen) in D-PBS (Gibco 14190, Invitrogen) to quantify the initial cell number in the cell culture chamber before the perfusion cell culture with various gradient combinations.

To generate TPZ gradients in the cell culture chamber, normal growth medium and the medium with TPZ are introduced into the bottom layer channel from two separate inlets. The generated TPZ gradients across the width of the cell culture chamber can be estimated by the simulation using the COMSOL Multiphysics software. For the oxygen gradient, the aforementioned experimental conditions are exploited for the drug testing. Four sets of experiments are conducted to demonstrate the device capability of generating perpendicular chemical and oxygen gradients for drug testing of cell viability, including: (1) Device A: cell culture with continuous normal growth medium perfusion with no gradients of TPZ and oxygen as control; (2) Device B: perfusion cell culture with only a TPZ gradient; (3) Device C: cell culture with continuous normal growth medium perfusion under an oxygen gradient; and (4) Device D: perfusion cell culture with both TPZ and oxygen gradients. During the experiments, the entire setup, including: microfluidic device and syringe pumps, is placed inside conventional cell incubators for optimal cell culture conditions. The microfluidic perfusion cell culture experiments last for 48 hours, and the experiments are repeated three times for statistical analysis. After the perfusion culture with various gradient combinations, the cells are stained with fluorescence live stain solution, Calcein AM (2  $\mu$ M) from LIVE/DEAD Viability/Cytotoxicity Kit (L3224, Invitrogen) in D-PBS (Gibco 14190, Invitrogen), to quantify the numbers of living cells in different portions within the cell culture chamber after the experiments. The cell number quantification is achieved by analyzing the captured fluorescence images using MetaMorph (Ver. 7.7.9.0, Molecular Devices, Sunnyvale, CA) software.

### 2.6. Cell migration study

Cell migration plays an essential role in many biological activities, it is associated with a variety of physiological processes such as: tissue formation, wound healing, and tumor invasion. It is important to study migration of interested cells under physiological microenvironments for biomedical researches. Therefore, the designed devices are further applied to study A549 cell migration under various combinations of chemokine and oxygen gradients. In the experiments, chemokine, stromal cell-derived factor (SDF-1 $\alpha$ ), is employed as a chemical stimulant for A549

cells. Growth medium (serum free) and the medium with SDF-1 $\alpha$  (300-28A, PreproTech, Rocky Hills, NJ)(100 ng/ml) are introduced into the bottom layer channel for two separate inlets with flow rates of 1  $\mu$ l/min to minimize the shear effect. For the oxygen gradient, the aforementioned experimental conditions are also exploited for the cell migration study.

To study the cell migration under various gradients, the microfluidic device is first treated with the ECM protein, fibronectin (F2006, Sigma-Aldrich Co., St Louis, MO), at a concentration of 100  $\mu$ g/ml for overnight inside the incubator before introducing the cell suspension into the microfluidic device. Cell suspensions for the experiments are made by centrifugation of dissociated cells at 1000 rpm for 3 min at room temperature, and the cells are resuspend in serum-free medium with final cell density of 2,000 cells/ $\mu$ l. 200  $\mu$ l of the A549 cells suspension is then pipetted into the cell culture chamber located at the bottom PDMS layer. The cells are then cultured under various gradient combinations, including: (1) Device A: cell culture with continuous normal growth medium perfusion with no gradients of SDF-1 $\alpha$  and oxygen as control; (2) Device B: perfusion cell culture with only a SDF-1 $\alpha$  gradient; (3) Device C: cell culture with continuous normal growth medium perfusion under an oxygen gradient; and (4) Device D: perfusion cell culture with both SDF-1 $\alpha$  and oxygen gradients, for 12 hours. The cell migration is observed by a live cell analyzer (JULI, NanoEnTek, Seoul, Korea) in real time (an image captured every 15 minutes), and the entire setup is placed inside a conventional cell incubator. The cell migration behaviors are characterized by analyzing the captured real-time bright field images using an image processing software, ImageJ (Ver. 1.47, National Institute of Health, Bethesda, MD) with Chemotaxis and Migration Tool (ibidi GmbH, Planegg, Germany). All the experiments are repeated three times for statistical analysis.

### **3. Results and discussion**

#### *3.1. Chemical gradient characterization*

To investigate the device performance for chemical gradient generation, fluorescein solution with concentration of 100  $\mu$ M and distilled water are introduced

into the device at flow rates of 1  $\mu\text{l}/\text{min}$  from left and right inlets, respectively. Fig. 2(b) shows the fluorescein concentration profiles estimated by measuring the fluorescence intensities within the cell culture chamber located in three different devices. The result shows that a fluorescein chemical gradient can be successfully established across the width of the cell culture chamber using the designed channel patterns. Furthermore, the experimentally measured gradient profile agrees well with the numerical simulated one with discrepancies less than 4.8  $\mu\text{M}$  across the entire cell culture chamber. The result suggests that the chemical gradients can be designed and well predicted using the simulation. In addition, the fluorescein gradient profiles at three positions from upstream to downstream are also analyzed. Fig. 2(c) shows the measured results which shows the three gradient profiles are similar to each other with differences less than 4.1  $\mu\text{M}$ . Consequently, the device can generate consistent chemical gradients through the entire cell culture chamber, which are desired for many cell culture applications.

### 3.2. Oxygen gradient characterization

To calibrate the generated oxygen gradients, the oxygen sensitive fluorescence dye is introduced into the channel at the bottom layer from both inlets at flow rate of 1  $\mu\text{l}/\text{min}$  to eliminate photobleaching during the measurements and simulate the cell culture experimental conditions. To quantitatively estimate the gradient profiles, fluorescence intensities of the dye within the measurement region in the cell culture chamber are first measured while air, pure nitrogen gas, and pure oxygen gas are flowed through the top layer channel as 20.9%, 0%, and 100% oxygen-saturated calibration data. Oxygen gradient profile generated using the spatially confined chemical reaction method then can be estimated using the Stern-Volmer equation<sup>23</sup>. In the experiments, pyrogallol solution (200 mg/ml) and NaOH (1 M) are introduced into the channel in the top layer at flow rates of 5  $\mu\text{l}/\text{min}$  for oxygen scavenging reaction. It is noted that only 7.2 ml of each chemical is required for a 24-hour experiment, which can minimize chemical consumptions and is suitable for long-term cell experiments.

Fig. 3(a) shows the average oxygen gradients profile by flowing pure nitrogen and oxygen gases into the top channel for calibration, and the gradient generated using the chemical reaction method within three different devices. The results demonstrate the oxygen gradients can be successfully generated using the chemical method, and the gradient is similar to that generated using the pure nitrogen gas. The oxygen tensions can be efficiently controlled due to the device designs, including: spatial confinement of the chemical reaction and the embedded PC film as a gas diffusion barrier. The comparison of the oxygen gradients generated inside the devices with and without the embedded PC film is shown in Fig. S1 in the Supporting Information. In the developed hybrid device, the oxygen tension can be lowered to about 1% at the upstream, and gradually increase to approximately 16% at the downstream in the measurement region. In addition, the oxygen gradients within left, middle and right 1/3 of the cell culture chamber in the measurement region are also characterized, and the results are shown in Fig. 3(b). The three oxygen gradient profiles are similar to each other, and the discrepancies are less than 1.8%. The results demonstrate consistent oxygen gradients can be generated using the developed method along the perfusion flow direction. It is noted that the oxygen gradients can be adjusted by controlling chemical reaction speeds using the chemicals (i.e. pyrogallol or NaOH) with different concentrations as shown in our previous study<sup>24</sup>.

### 3.3. Drug testing

The cell compatibility of the device is first confirmed before the drug testing in the experiments. Fig. 4 shows the microscopic images of A549 cells right after seeding into the device, and after initial 24-hour culture inside the device. Fig. 4(b) shows that the cells can adhere well on the substrate. The cell morphology further indicates great biocompatibility of the designed devices. In order to quantitatively evaluate the cell viability after the initial culture, the cells are stained with live (green)/dead (red) stain after the 24-hour culture. Fig. 4(b) shows the fluorescence image of the stained cells. The image suggests the cells have high viability (> 99.0%) after the 24-hour culture before gradient experiments. Therefore, in the drug testing experiments, cells are assumed to be alive before the experiments for the analysis. In the gradient experiments, cells are stained with CellTracker™ Blue for cell number

estimation right before application of the gradients for the drug testing. The counted cell numbers are taken as the live cell numbers before the experiments.

In the drug testing experiments, hypoxia-activated anti-cancer drug (TPZ) gradients are generated across the cell culture as shown in Fig. 5(a). TPZ dissolved in normal growth medium with final concentration of 200  $\mu\text{M}$  and normal growth medium are introduced into the device at flow rates of 1  $\mu\text{l}/\text{min}$  from left and right inlets, respectively. The low flow rate can minimize the shear effect to the cells cultured inside the device. The generated TPZ gradient is numerically simulated using the COMSOL Multiphysics. The simulated gradient profile is plotted as Fig. 5(b), and the average TPZ concentrations within left, middle, and right 1/3 of the cell culture chamber in the measurement region are shown in Fig. 5(a). The results show that the average TPZ concentrations are 166.5, 101.0, and 26.8  $\mu\text{M}$  within the left, middle, and right portions of the cell culture chamber, respectively. As a result, the cells can experience chemicals with different concentrations inside the device across the width of the cell culture chamber. For the oxygen gradient, the average oxygen tensions within the up-, mid-, and downstream portions are 3.8, 9.6, and 13.6%, respectively. Therefore, the cells can be cultured under different oxygen tensions as shown in Fig. 5(a).

After 48-hour drug testing, Fig. 5(c) shows fluorescence images of the A549 cells stained with live stain (Calcein AM) within the measurement regions after 48-hour gradient experiments, and heat maps demonstrating live cell ratios in different portions of the cell culture chamber inside measurement regions. The live cell ratio is defined as a ratio of live cell numbers before the experiments (CellTracker<sup>TM</sup> Blue stained cells) to live cell numbers after the experiments (Calcein AM stained cells). A statistical analysis, one-way ANOVA with Tukey's test, is also performed for each device to study the differences of live cell ratios within the cell culture chamber. The fluorescence images show different live cell distributions within the measurement regions under various gradient combinations. In Devices A (control – no gradients) and C (with only oxygen gradient), live cells uniformly distributed through the entire measurement regions. The heat maps also show that there are no statistical differences among different portions inside the measurement region of each device of

A and C, and all the live cell ratios are greater than 120%, which indicates the cells in these two devices not only survive but also well proliferate during the 48-hour experiments. The average live cell ratio within the entire measurement region of Device C is slightly lower than that of Device A, which may result from the longer set up time of Device C outside the incubators. However, there are no statistical differences ( $p > 0.05$ , unpaired, two-tailed Student's t-tests) between two ratios calculated from entire measurement regions of Device A and C, which confirm that chemical reaction method exploited for generation of oxygen gradient in the experiments is cell compatible. In Device B, cells experience TPZ concentrations ranging from 185  $\mu\text{M}$  (left) to 10  $\mu\text{M}$  (right) across the width of the cell culture chamber under normoxia ( $\sim 20\%$   $[\text{O}_2]$ ) condition. The fluorescence image as shown in Fig. 5(c) indicates more live cells on the right side than left side within the cell culture chamber in Device B, which results from the intrinsic cytotoxicity of TPZ even under normoxia. In addition, the heat map shows higher live cell ratios on the right side (average 108.8% with average TPZ concentration of 26.8  $\mu\text{M}$ ) than left side (average 36.8% with average TPZ concentration of 166.5  $\mu\text{M}$ ), and no statistical difference between up-, mid-, and downstream in all left, middle, and right portions. The results suggest the developed device can successfully generate stable chemical (TPZ) gradients through the cell culture chamber for cell studies.

Moreover, the cells experience both TPZ gradients and oxygen gradients, ranging from 1.7% (upstream) to 16.7% (downstream), within a measurement region in Device D. The fluorescence image as shown in Fig. 5(c) indicates less live cells on the left top corner than other portions within the cell culture chamber in Device D, which results from hypoxia activated cytotoxicity of TPZ. In the heat map, the live cell ratios are higher on the right portions than left portions at the same position across the width of cell culture chamber due to the lower TPZ concentration on the right side. In the same position along the perfusion flow direction, the live cell ratio is lower in the upstream than downstream due to the hypoxia-activated cytotoxicity of TPZ. For example, in the middle portion of the chamber, the live cell ratio increases from 5.9% in the upstream (with average oxygen tension of 3.8%) to 33.4% in the downstream (with average oxygen tension of 13.6%). More than 5.6 times difference in the live cell ratios suggests oxygen can greatly affect the drug efficiency due to its

mode of action. The results demonstrate the developed device can successfully generate perpendicular chemical (TPZ) and oxygen gradients within the cell culture chamber to evaluate cell viability for drug testing. Using the developed device, drug efficiency under different oxygen tensions can be evaluated in a high throughput manner. In addition, the results indicate the importance of oxygen tensions in various biomedical studies, including drug testing as demonstrated in the experiments.

### 3.4. Cell migration study

Cell migration study is also performed using the device to investigate A549 cell migration patterns with the presence of chemokine and oxygen gradients. In order to estimate the chemokine gradient within the cell culture chamber, COMSOL Multiphysics is employed to numerically simulate the generated SDF-1 $\alpha$  gradient. The simulated gradient profile is plotted as Fig. 6(a), and the result shows that the SDF-1 $\alpha$  concentrations ranges from 1.0 to 11.2  $\mu$ M across the width of the cell culture chamber. Fig. 6(b) shows the bright field images recorded by the live cell analyzer before and after a migration experiment with both chemokine and oxygen gradients. The migration paths of cells are analyzed using the ImageJ software through the time-lapsed images.

Fig. 7(a) shows the analyzed cell migration paths of one set of experiments with four different gradient combinations (Device A, B, C and D). In the plots, the blue circles indicate the average migration movements after 12-hour experiments of randomly selected 10 cells cultured in each cell culture chamber. In Devices A (control – no gradients), the average movements of cell migration in both axes are less than 4  $\mu$ m during the 12-hour experiment. The result suggests that the cells migrate randomly without specific directionalities when no gradients present, and it also shows the continuous medium perfusion with the low flow rate does not affect cell migration within the device. In contrast, in Device B (with only SDF-1 $\alpha$  gradient) and C (with only oxygen gradient), the average movements of cell migration show specific directionalities. With the SDF-1 $\alpha$  gradient in Device B, the cells tend to migrate toward to the direction with higher chemokine concentration, which suggests the SDF-1 $\alpha$  acts as a chemo attractant for A549 cells. This SDF-1 $\alpha$  chemotaxis



effect has been discussed in previous papers<sup>37,38</sup>. Therefore, the result confirms that the developed device is capable of generating stable chemical gradients for cell studies. In Device C, the average movement of cell migration indicates the A549 cells tend to migrate toward low oxygen tension side (upstream). To the best of our knowledge, such aerotactic behavior of mammalian cells has not been studied in literatures due to the instrumental limitations. Taking advantage of the hybrid structure and the spatially confined oxygen scavenging chemical reaction method, the local spatial distribution of oxygen tensions can be efficiently controlled and stably maintained. Consequently, the developed device provides a reliable platform to study cell migration under oxygen gradients. Interestingly, with both chemokine and oxygen gradients in Device D, A549 cells move toward low oxygen side (upstream) without significant movement toward high SDF-1 $\alpha$  concentration side (left). This novel finding suggests oxygen gradients may play more important roles in guiding cell migration than chemokine gradients.

In order to quantitatively evaluate the directionality of the migration, chemotactic index and aerotactic index are calculated in the analysis. The index is defined as the displacement of a cell migrates in the direction parallel to the gradient divided by the total distance the cell travels, and a cell migrates toward high concentration area is defined as positive direction as shown in Fig. 7(b)<sup>39</sup>. Fig. 7(c) and (d) show the calculated chemotactic and aerotactic index for each device from three independent experiments, respectively. In Fig. 7(c), average chemotactic index for cells cultured in Device A, C, and D are close to zero (absolute numbers are less than 0.02), showing the cells migrate randomly in X-axis even with SDF-1 $\alpha$  gradient in Device D. The one-way ANOVA assay is performed to evaluate the statistical difference for cell migration on each device. The A549 cells cultured in the Device B are the only populations with average chemotactic index (0.29) being statistically different from the control case (Device A) due to the chemotaxis effect. In contrast, average aerotactic index are close to zero (absolute numbers less than 0.04) only when oxygen gradients are absent (Device A and B). Comparing to control (Device A), cells cultured in Device C and D tend to migrate toward low oxygen sides with average aerotactic index of -0.28 and -0.24, respectively, regardless of the presence of the chemokine gradient. In addition, the discrepancy between the aerotactic index

calculated in Device C and D is statistically insignificant. The results suggest that aerotaxis effect of cells may play more important roles in cell migration than chemotaxis effect under certain physiological conditions. Furthermore, the results demonstrate the chemotaxis and aerotaxis effects of A549 cells cultured under chemokine (SDF-1 $\alpha$ ) and oxygen gradients cannot be simply superposed. Oxygen tension and its gradient may play an essential role in regulating ligand (CXCL12) and receptor (CXCR4) binding and further affect cell migration<sup>40</sup>. Further study of cell migration under various gradient combinations using the developed the device as demonstrated in this paper can pave a way to better understand various important *in vivo* biological activities, including: cancer metastasis and wound healing.

#### 4. Conclusion

This paper reports a novel microfluidic device capable of simultaneously generating perpendicular chemical and oxygen gradients for *in vitro* cell culture studies using the PDMS-PC hybrid structure. Taking advantages of microfluidics, chemical gradients are generated using a series of parallel-arranged serpentine channels for chemical mixing. The oxygen gradients are generated using the spatially confined chemical reaction method developed in our previous papers, which makes the device requires small amounts of chemicals and syringe pumps to operate. Also, the device can be directly used inside conventional cell incubators. Therefore, the entire device can be set up with minimal instrumentation, which makes the device more practical to be used in biological labs. In the experiments, the drug testing and the cell migration study are performed to demonstrate the novel functionalities of the device. The experimental results show that the device can successfully generate stable perpendicular chemical and oxygen gradients for cell studies, which may help biologists to better study cellular responses under gradient combinations that do exist in physiological microenvironments. Furthermore, the cell migration study demonstrates the aerotactic behavior of the mammalian A549 cells, suggesting oxygen gradient may play a key role in regulating cell migrations, which has not yet been carefully studied in the existing literatures. Also, the results show that the cell migration behaviors under combinations of chemokine and oxygen gradients cannot be simply superposed from the single gradient results. With the demonstrated results,

the developed microfluidic device shows great promise and advantages for various *in vitro* cell biology studies for biomedical applications.

### Acknowledgements

This paper is based on work supported by the National Health Research Institutes (NHRI) in Taiwan under Career Development Grant (CDG) (EX103-10021EC), the Taiwan National Science Council (NSC 101-2628-E-001-002-MY3), and the Academia Sinica Research Program in Nanoscience and Nanotechnology.

### References

1. J. E. Phillips, K. L. Burns, J. M. Le Doux, R. E. Guldberg and A. J. García, *Proceedings of the National Academy of Sciences*, 2008, 105, 12170-12175.
2. F. Wang, *Cold Spring Harbor Perspectives in Biology*, 2009, 1.
3. C.-W. Chang and M.-J. Wang, *ACS Sustainable Chemistry & Engineering*, 2013, 1, 1129-1134.
4. S. H. Oh, C. L. Ward, A. Atala, J. J. Yoo and B. S. Harrison, *Biomaterials*, 2009, 30, 757-762.
5. M. Decaris, C. Lee, M. Yoder, A. Tarantal and J. K. Leach, *Angiogenesis*, 2009, 12, 303-311.
6. Millhorn DE, Raymond R, Conforti L, Zhu W, Beitner-Johnson D, Filisko T, Genter MB, Kobayashi S and P. M., *Kidney Int.*, 1997, 51, 527-535.
7. S. Sant, M. J. Hancock, J. P. Donnelly, D. Iyer and A. Khademhosseini, *The Canadian Journal of Chemical Engineering*, 2010, 88, 899-911.
8. Y. Du, J. Shim, M. Vidula, M. J. Hancock, E. Lo, B. G. Chung, J. T. Borenstein, M. Khabiry, D. M. Cropek and A. Khademhosseini, *Lab on a Chip*, 2009, 9, 761-767.
9. M. Adler, M. Polinkovsky, E. Gutierrez and A. Groisman, *Lab on a Chip*, 2010, 10, 388-391.
10. J. Pihl, J. Sinclair, E. Sahlin, M. Karlsson, F. Petterson, J. Olofsson and O. Orwar, *Analytical Chemistry*, 2005, 77, 3897-3903.
11. D. Huh, H. Fujioka, Y.-C. Tung, N. Futai, R. Paine, J. B. Grothberg and S. Takayama, *Proceedings of the National Academy of Sciences*, 2007, 104, 18886-18891.
12. A. Shamloo, N. Ma, M.-m. Poo, L. L. Sohn and S. C. Heilshorn, *Lab on a Chip*, 2008, 8, 1292-1299.
13. Y. Kamotani, T. Bersano-Begey, N. Kato, Y.-C. Tung, D. Huh, J. W. Song and S. Takayama, *Biomaterials*, 2008, 29, 2646-2655.
14. J. W. Song, S. P. Cavnar, A. C. Walker, K. E. Luker, M. Gupta, Y.-C. Tung, G. D. Luker and S. Takayama, *PLoS ONE*, 2009, 4, e5756.
15. S. Kim, H. J. Kim and N. L. Jeon, *Integrative Biology*, 2010, 2, 584-603.
16. N. J. Douville, P. Zamankhan, Y.-C. Tung, R. Li, B. L. Vaughan, C.-F. Tai, J. White, P. J. Christensen, J. B. Grothberg and S. Takayama, *Lab on a Chip*, 2011, 11, 609-619.

17. M.-C. Liu, H.-C. Shih, J.-G. Wu, T.-W. Weng, C.-Y. Wu, J.-C. Lu and Y.-C. Tung, *Lab on a Chip*, 2013, 13, 1743-1753.
18. A. Y. Hsiao, Y.-s. Torisawa, Y.-C. Tung, S. Sud, R. S. Taichman, K. J. Pienta and S. Takayama, *Biomaterials*, 2009, 30, 3020-3027.
19. L. L. Bischel, E. W. K. Young, B. R. Mader and D. J. Beebe, *Biomaterials*, 2013, 34, 1471-1477.
20. O. F. Khan and M. V. Sefton, *Biomaterials*, 2010, 31, 8254-8261.
21. B. G. Chung, L. A. Flanagan, S. W. Rhee, P. H. Schwartz, A. P. Lee, E. S. Monuki and N. L. Jeon, *Lab on a Chip*, 2005, 5, 401-406.
22. J. F. Lo, E. Sinkala and D. T. Eddington, *Lab on a Chip*, 2010, 10, 2394-2401.
23. Y.-A. Chen, A. D. King, H.-C. Shih, C.-C. Peng, C.-Y. Wu, W.-H. Liao and Y.-C. Tung, *Lab on a Chip*, 2011, 11, 3626-3633.
24. C.-C. Peng, W.-H. Liao, Y.-H. Chen, C.-Y. Wu and Y.-C. Tung, *Lab on a Chip*, 2013, 13, 3239-3245.
25. L. Wang, W. Liu, Y. Wang, J.-c. Wang, Q. Tu, R. Liu and J. Wang, *Lab on a Chip*, 2013, 13, 695-705.
26. O. Trédan, C. M. Galmarini, K. Patel and I. F. Tannock, *Journal of the National Cancer Institute*, 2007, 99, 1441-1454.
27. Y. Xia and G. M. Whitesides, *Annual Review of Materials Science*, 1998, 28, 153-184.
28. Y.-H. Chen, C.-C. Peng, Y.-J. Cheng, J.-G. Wu and Y.-C. Tung, *Biomechanics*, 2013, 7, -.
29. N. L. Jeon, S. K. W. Dertinger, D. T. Chiu, I. S. Choi, A. D. Stroock and G. M. Whitesides, *Langmuir*, 2000, 16, 8311-8316.
30. K. Funamoto, I. K. Zervantonakis, Y. Liu, C. J. Ochs, C. Kim and R. D. Kamm, *Lab on a Chip*, 2012, 12, 4855-4863.
31. L. F. Fieser, *Journal of the American Chemical Society*, 1924, 46, 2639-2647.
32. J.-C. Lu, W.-H. Liao and Y.-C. Tung, *Journal of Micromechanics and Microengineering*, 2012, 22.
33. G. Mehta, J. Lee, W. Cha, Y.-C. Tung, J. J. Linderman and S. Takayama, *Analytical Chemistry*, 2009, 81, 3714-3722.
34. W. Zhong, P. Urayama and M.-A. Mycek, *Journal of Physics D: Applied Physics*, 2003, 36, 7.
35. W. L. Wouters BG, Brown JM, *Annals of Oncology*, 1999, 10, 5.
36. L. Marcu and I. Olver, *Current Clinical Pharmacology*, 2006, 1, 71-79.
37. R. J. Phillips, M. D. Burdick, M. Lutz, J. A. Belperio, M. P. Keane and R. M. Strieter, *American Journal of Respiratory and Critical Care Medicine*, 2003, 167, 1676-1686.
38. J. Yang, B. Zhang, Y. Lin, Y. Yang, X. Liu and F. Lu, *Cancer Letters*, 2008, 269, 46-56.
39. A. Shamloo, M. Manchandia, M. Ferreira, M. Mani, C. Nguyen, T. Jahn, K. Weinberg and S. Heilshorn, *Integrative Biology*, 2013, 5, 1076-1085.
40. Y.-J. Seo, S. H. Koh, H. J. Kang, H. Y. Shin, G. Jeong and H. S. Ahn, *Biochemical and Biophysical Research Communications*, 2007, 364, 388-394.

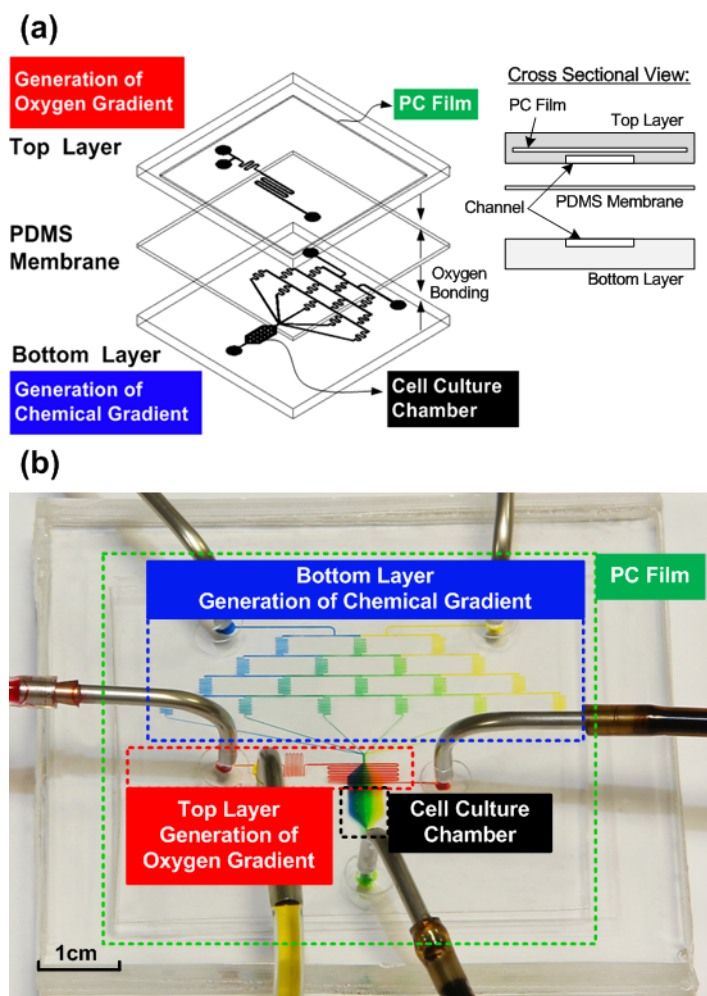


Fig. 1. (a) Schematic and fabrication process of the developed PDMS microfluidic device capable of generating perpendicular chemical and oxygen gradients. (b) Photo of the fabricated device filled with colored food dyes.

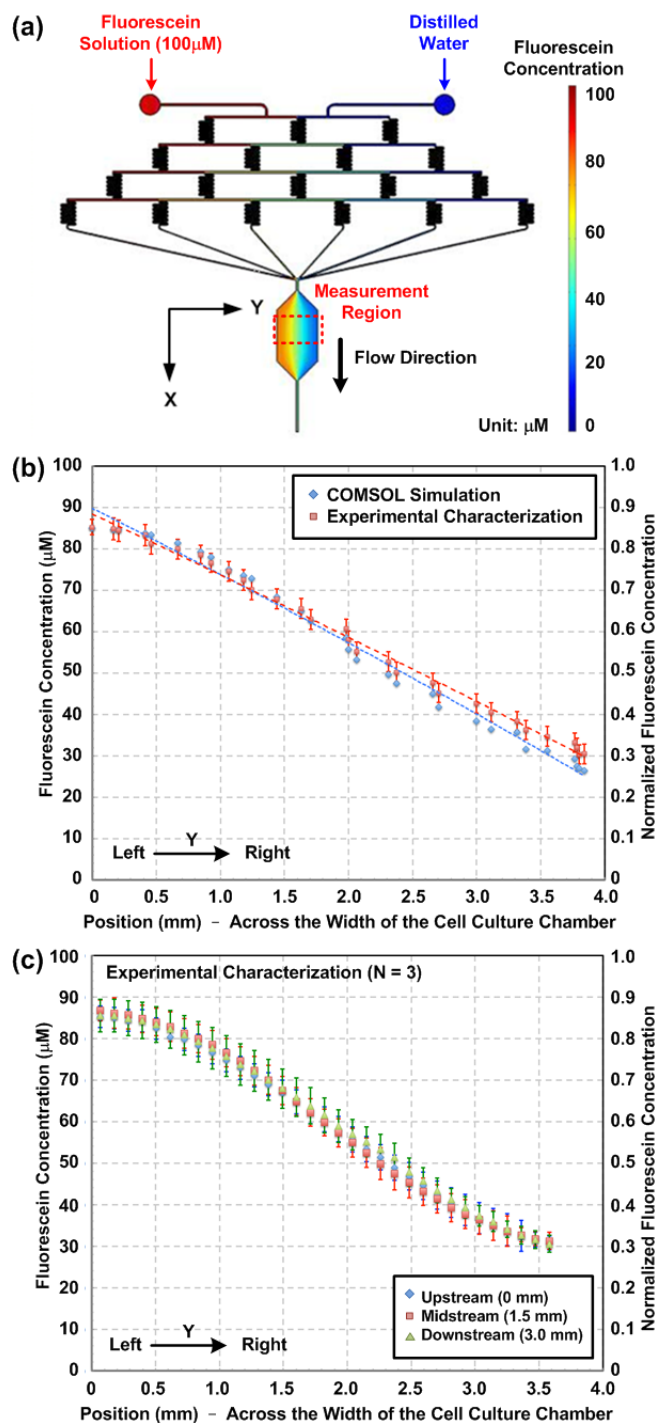


Fig. 2. (a) Chemical concentration profile simulated using COMSOL Multiphysics when introducing fluorescein solution ( $100 \mu\text{M}$ ) and distilled water into the device at flow rates of  $1 \mu\text{l min}^{-1}$  from the left and right inlet, respectively. The generated chemical gradient is perpendicular to the flow direction (Y-axis), and the generated oxygen gradient is along the flow direction (X-axis). (b) Comparison of fluorescein gradients across the width of the cell culture chamber obtained from simulation and experimental characterization under same conditions. (c) Fluorescein gradients across the width of the cell culture chamber measured at up-, mid-, and downstream inside the cell culture chamber. The data are expressed as the mean  $\pm$  SD ( $N = 3$ ).

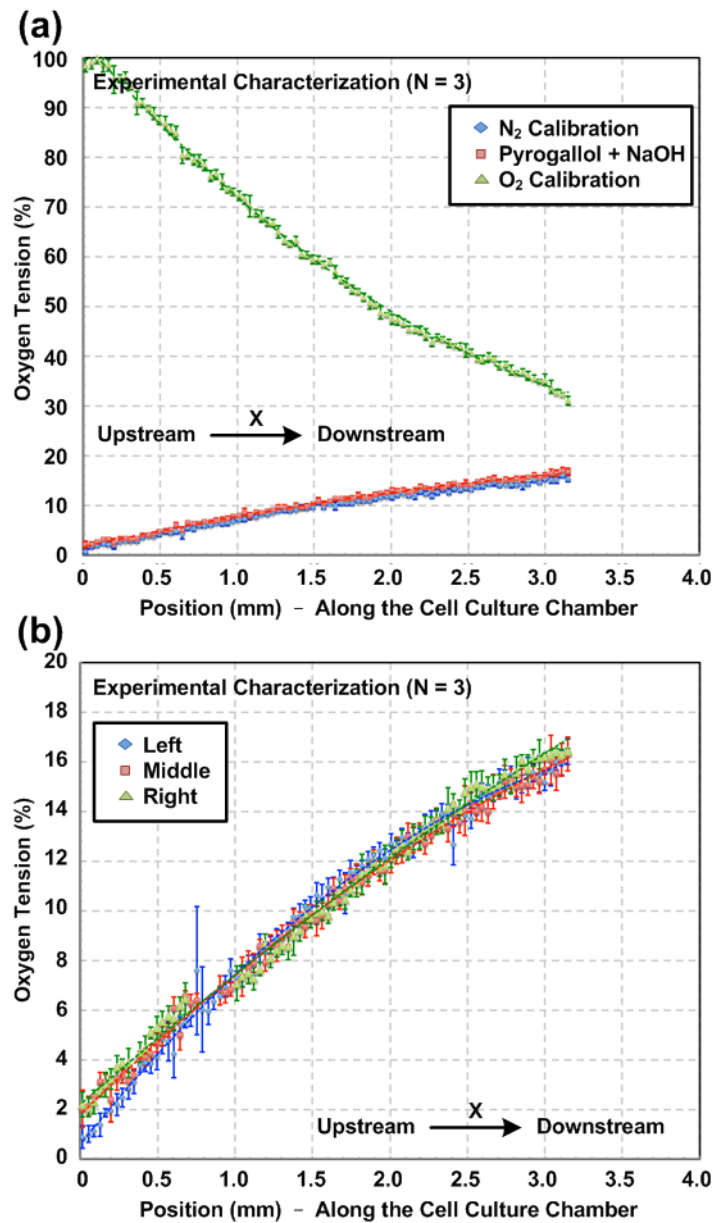


Fig. 3. (a) The experimentally measured oxygen gradients when introducing pure nitrogen and oxygen gases for calibration, and the gradient obtained using the spatially confined chemical reaction (pyrogallol+NaOH) method. (b) Comparison of the experimentally characterized oxygen gradients in the left, middle, and right portions within the cell culture chamber using the spatially confined chemical reaction method. The data are expressed as the mean  $\pm$  SD (N = 3).

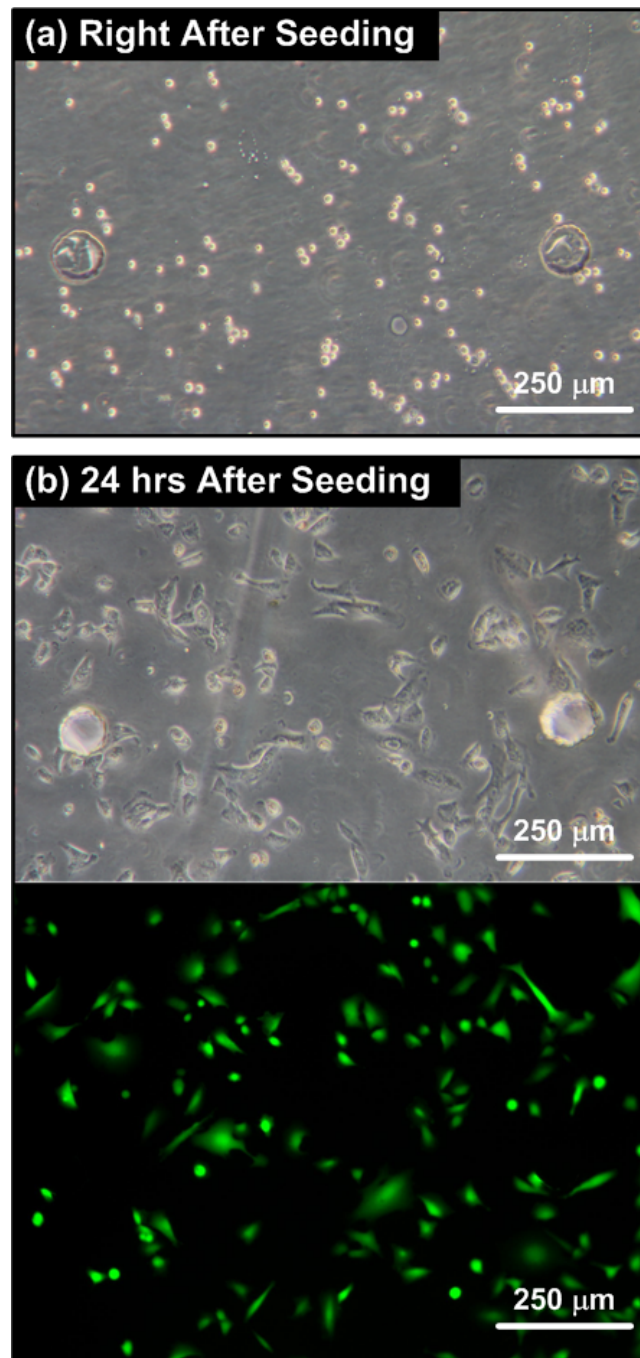


Fig. 4. The bright field and fluorescence microscopic images of the A549 cells (a) right after seeding, and (b) after 24-hour culture inside the microfluidic device. After 24-hour culture, the A549 can attach well on the cell culture chamber substrate. The fluorescence image (live/dead stain) shows that most of the cells are live ( $> 99.0\%$ ) after the seeding and initial culture process.



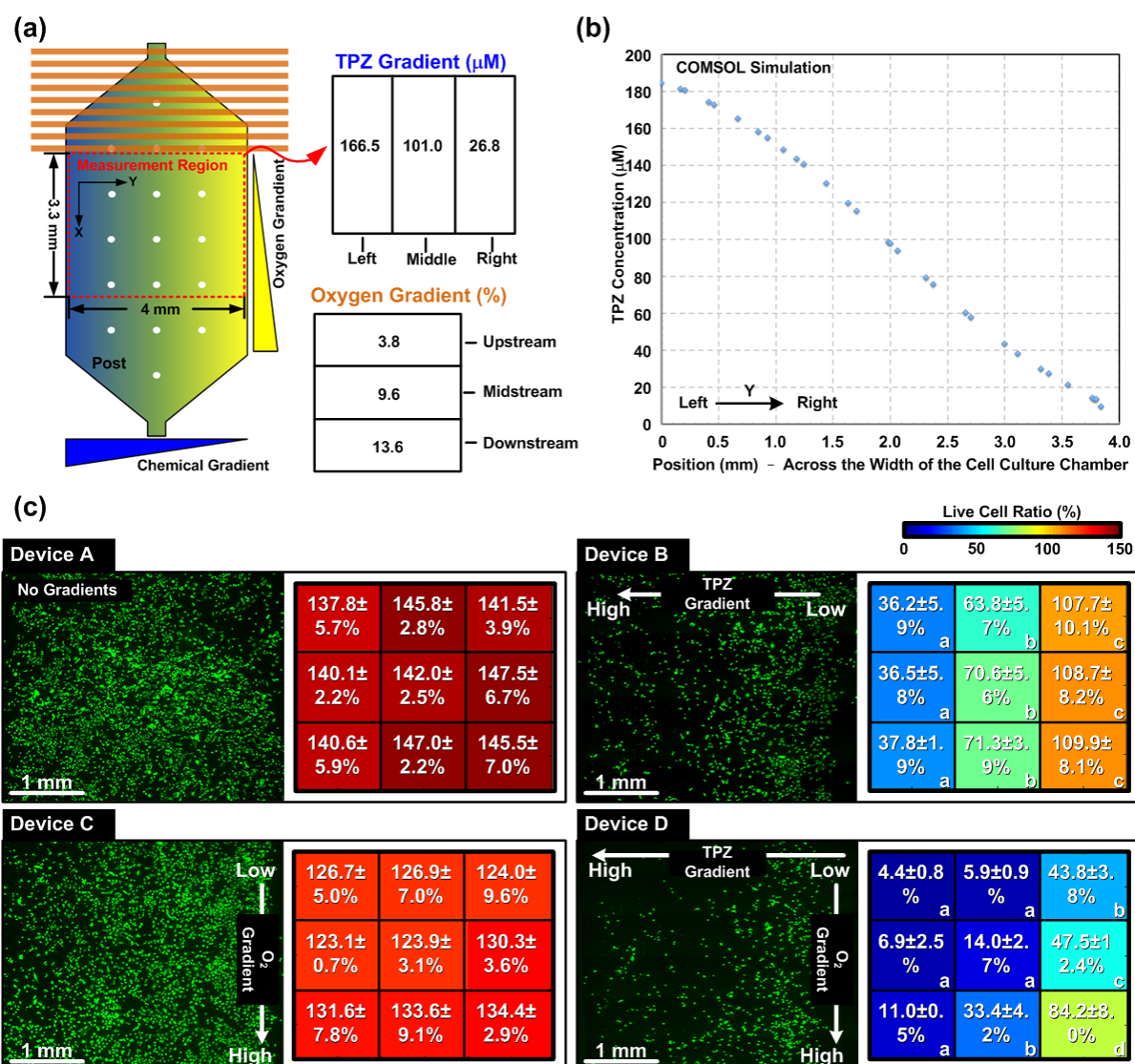


Fig. 5. (a) Measurement region (4 mm in width; 3.3 mm in length) within the cell culture chamber during the experiments. The insets show the numerically simulated average chemical (TPZ) concentrations and the experimentally characterized average oxygen tensions in different portions within the measurement region. (b) TPZ gradient across the width of the cell culture chamber obtained from COMSOL Multiphysics simulation for the drug testing. (c) Fluorescence images of A549 cells inside the cell culture chambers located within the measurement regions after 48-hour culture under 4 different gradient combinations (Device A, B, C, and D). The cells are stained with live stain (green) for live population estimation after the experiments. The right panels show the heat maps of the live cell ratios in the different portions within the measurement regions (N = 3). In each heat map, different letters between portions represent a significant difference in live cell ratios (a, b, c, d = p<0.05) in a device, and the data are expressed as the mean  $\pm$  SD.

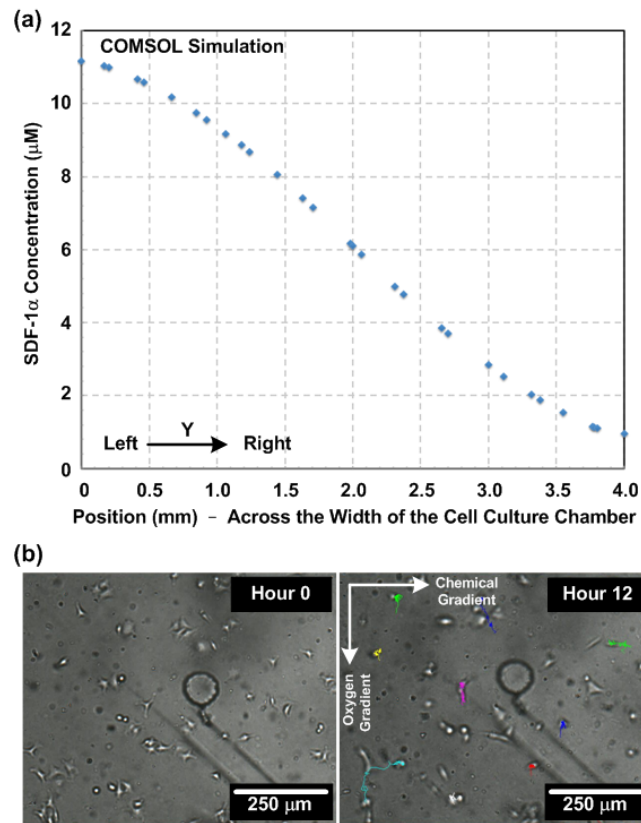


Fig. 6. (a) SDF-1 $\alpha$  gradient across the width of the cell culture chamber obtained from COMSOL Multiphysics simulation for the cell migration study. (b) Bright field images of the A549 cells before and after 12-hour migration experiment inside the microfluidic device with perpendicular chemical (SDF-1 $\alpha$ ) and oxygen gradients.

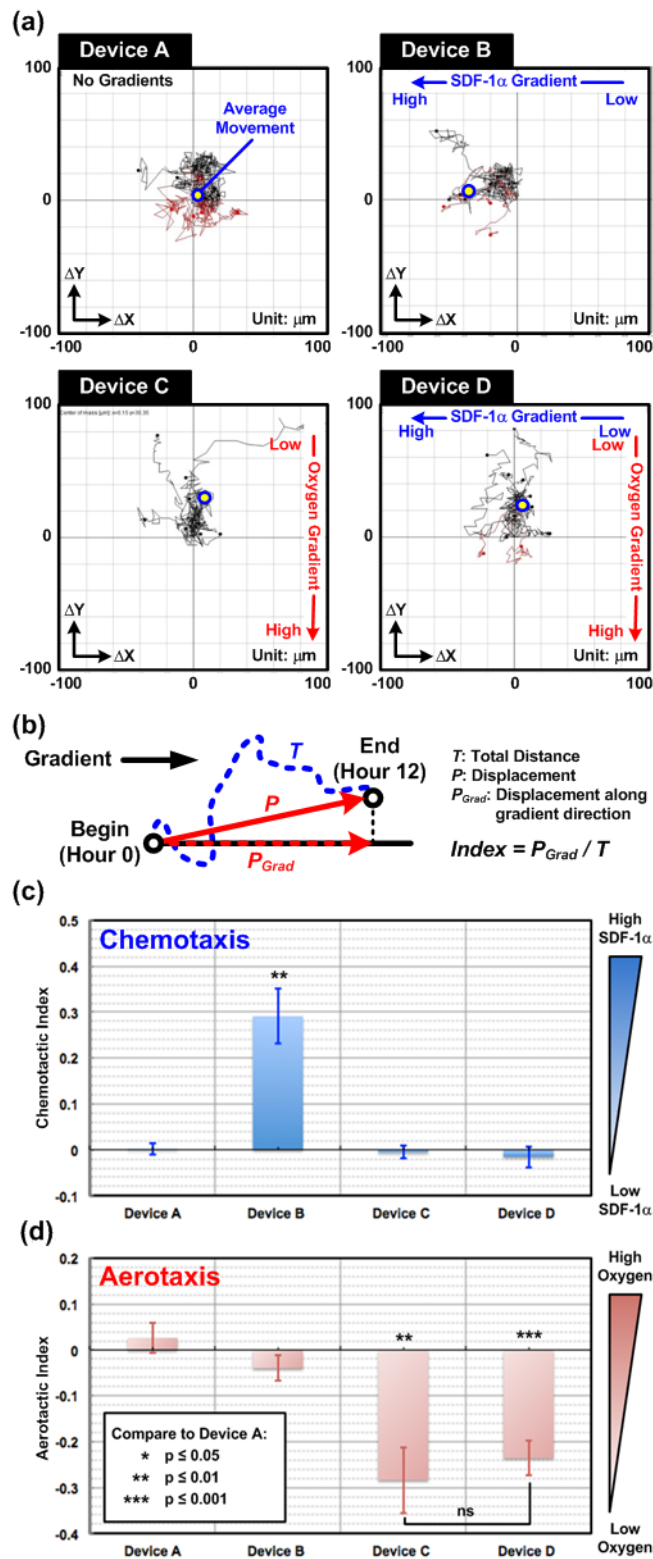


Fig. 7. (a) A549 cell migration paths under 4 different gradient combinations (Device A, B, C, and D) during 12-hour culture inside the devices. (b) Illustration of the definition of chemotactic/aerotactic index. (c) Chemotactic index for the A549 cells migrate under 4 different combinations, and the data are expressed as the mean  $\pm$  SD (N = 3; n = 10 for each experiment). (d) Aerotactic index for the A549 cells migrate under 4 different combinations, and the data are expressed as the mean  $\pm$  SD (N = 3; n = 10 for each experiment).